NASA Technical Memorandum 104640

# Estimating the Thickness of Sea Ice Snow Cover in the Weddell Sea from Passive Microwave Brightness Temperatures

K. R. Arrigo
*NASA Goddard Space Flight Center*
*Greenbelt, Maryland*

G. L. van Dijken
*Department of Oceanography*
*Texas A&M University*
*College Station, Texas*

J. C. Comiso
*NASA Goddard Space Flight Center*
*Greenbelt, Maryland*


National Aeronautics and
Space Administration

**Goddard Space Flight Center**
Greenbelt, Maryland 20771

**1996**

This publication is available from the NASA Center for AeroSpace Information,
800 Elkridge Landing Road, Linthicum Heights, MD 21090-2934, (301) 621-0390.

# Estimating the Thickness of Sea Ice Snow Cover in the Weddell Sea from Passive Microwave Brightness Temperatures

**K. R. Arrigo, G. L. van Dijken, and J. C. Comiso**

## ABSTRACT

Passive microwave satellite observations have frequently been used to observe changes in sea ice cover and concentration. Comiso et al. (1989) showed that there may also be a direct relationship between the thickness of snow cover ($h_S$) on ice and microwave emissivity at 90 GHz. Because the in situ experiment of Comiso et al. (1989) was limited to a single station, the relationship is re-examined in this paper in a more general context and using more extensive in situ microwave observations and measurements of $h_S$ from the Weddell Sea 1986 and 1989 winter cruises. Good relationships were found to exist between $h_S$ and the emissivity at 90 GHz–10 GHz and the emissivity at 90 GHz–18.7 GHz when the standard deviation of $h_S$ was <50% of the mean and when $h_S$ was <0.25 m. The reliance of these relationships on $h_S$ is most likely caused by the limited penetration through the snow of radiation at 90 Ghz. When the algorithm was applied to Special Sensor Microwave/Imager (SSM/I) satellite data from the Weddell Sea, the resulting mean $h_S$ agreed within 5% of the mean calculated from >1400 in situ observations.

## INTRODUCTION

The emissivity of sea ice and its associated snow cover is much greater at some microwave frequencies than those of seawater. Consequently, passive microwave sensors have proven to be very useful for mapping the extent of the sea ice cover. To date, several sensors have been launched aboard satellites and have provided a nearly continuous record of sea ice distribution since 1972. These include the single band Electrically Scanning Microwave Radiometer (ESMR, Nimbus-5 satellite, 1972-1977), the Scanning Multichannel Microwave Radiometer (SMMR, Nimbus-7 satellite, 1978-1987) with bands at 5 frequencies (6, 10, 18, 21, and 37 GHz) at dual, horizontal (H) and vertical (V) polarization, and the Special Sensor Microwave/Imager (SSM/I, Defense Meteorological Satellite Program, 1987-present), a radiometer with frequencies at 19 GHz (H and V polarization), 37 GHz (H and V polarization), 85 GHz (H and V polarization), and 22 GHz (V polarization only). The spatial resolution of these sensors is approximately 30 $km^2$.

In order to provide in situ measurements which can be compared with satellite observations, Comiso et al. (1989) used surface-based sensors to measure local variability in the microwave signature of sea ice in the Weddell Sea. Comiso et al. (1989) also examined the effect of snow thickness on the emission of microwaves. To do so, they mounted a radiometer ~1.5 m. above the sea ice in an area of substantial snow cover. Radiometric measurements were made of the snow surface when it was undisturbed and as the snow was carefully scraped off in layers of 0.05 m. Significant increases in brightness temperature ($T_B$) at 90 GHz were observed when the snow was removed, while at other frequencies the signal remained relatively constant (Fig. 1). Comiso et al. (1989) demonstrated a nearly linear decrease in $T_B$ with increasing $h_s$ at 90 GHz (V) when the instrument was oriented 50° from nadir, the approximate viewing angle of the SSM/I. This suggested that it might be feasible to estimate the thickness of snow cover within the ice pack using satellite mounted sensors.

The decrease in $T_B$ at 90 GHz with increasing $h_s$ has been postulated as caused by greater attenuation of radiation emitted from the snow/ice interface by the thicker snow pack. It was argued by Comiso et al. (1989) that the absence of the decrease in $T_B$ at lower frequencies was because of the smaller influence of volume scattering on $T_B$, since the wavelengths are large compared to the size of the snow particles. Modeling results of the effect of snow cover on sea ice show similar behavior. It must be noted, however, that the microwave signal is not only influenced by $h_s$ but by other characteristics of the snow pack as well, such as the wetness, granularity, density, and presence of informalities like ice lenses, as well as the underlying sea ice itself.

Unfortunately, the preliminary findings reported by Comiso et al. (1989) were limited to only a few measurements made at a single location. The objective of the present study is to re-examine the relationship between $h_S$ and its associated microwave signature using surface-based data, and if possible, to develop an algorithm appropriate for estimating $h_S$ from space. The surface-based data used in this study were collected during the cruises ANT V/2 (1986) and ANT VIII/2 (1989) to the Weddell Sea aboard the R/V Polarstern. Also, satellite TBs are correlated with in situ snow measurements where no ship observations were available.

ANT V/2 (1986)

Observations of both $h_S$ and microwave $T_B$ were made during the 1986 Winter Weddell Sea Project at 32 out of a total of 37 stations. A ship-mounted radiometer was positioned approximately 17 m above the sea ice and measured $T_B$ at frequencies of 6, 10, 18.7, 37, and 90 GHz at various angles from nadir. The change in polarization from vertical to horizontal were made by rotating the antenna 90°. Only data measured at an angle 50° from nadir were used in the present study, because this is the approximate angle at which SSM/I data are collected (i.e., 53°).

The mean value for $h_S$ at each of the 32 stations was determined from about 26 individual measurements. The mean value for $h_S$ for all stations ranged from 0 to 0.4 m, with 3 stations having $h_S = 0$ m, 27 stations with $h_S < 0.25$ m and 2 stations with $h_S > 0.25$ m (0.26 and 0.40 m). The standard deviation of $h_S$ ranged from 20-130% of the mean.

Emissivity ($\varepsilon$) at the sea ice surface, calculated as

$$\varepsilon = \frac{T_B - T_{sky}}{T_I - T_{sky}}$$

(Comiso et al 1989), was highly correlated with $T_B$ in the 1986 data (Fig. 2), where $T_I$ is the snow-ice interface temperature and $T_{sky}$ is the radiance caused by the atmosphere and free space. For example, the regression of $T_B$10 GHz (V and H polarization) against $\varepsilon$10 GHz (V and H polarization) at the same station yielded a correlation coefficient of >0.99 (Fig. 2A). This was also true at 90 GHz (V and H polarization) (Fig. 2B).

A plot of $\varepsilon$90 GHz (V) versus $\varepsilon$8.7 GHz (V) (Fig. 3) illustrates that the latter is reduced at $h_S$=0 m (i.e., the three data points in the lower right quadrant). When snow was present on the surface of the sea ice, the signal at 18.7 GHz remained approximately constant, while the micro-wave signal at 90 GHz varied from 0.75 to 0.98 (Fig. 3). This relationship was shown previously by

Comiso et al. (1989) who attributed the variability at 90 GHz to differences in either $h_S$ or properties of the snow cover. A similar relationship also was apparent when the 90 Ghz ($\varepsilon$ and $T_B$, V and H polarization) band was plotted against 10 or 37 GHz bands, but not the 6 GHz band which exhibited more scatter.

Plots of $h_S$ versus $\varepsilon$ or $T_B$ at 6, 10 (Fig. 4A), 18.7, and 37 GHz remained relatively flat (no slope), indicating that there was little sensitivity in the passive microwave signal at these frequencies to variation in $h_S$ within the snow pack. The obvious exception was the case where $h_S$=0 m which exhibited much lower values for both $\varepsilon$ and $T_B$. On the other hand, the 90 GHz (V) frequency exhibited much greater variability with respect to $h_S$, although there was no significant correlation between the signal at 90 GHz and $h_S$ (Fig. 4B).

However, when stations where the standard deviation of $h_S$ was greater than 50% of the mean were removed from the analyses, the relationship between $\varepsilon$90 GHz (V) and $h_S$ improved dramatically (Fig. 5). Two types of outliers in Fig. 5 can be identified; stations where $h_S = 0$ m (n = 2) and stations where $h_S > 0.25$ m (n = 2). When those stations were omitted, a good linear relationship between $h_S$ and the 90 GHz (V) frequency was obtained (Fig. 7). The equations and goodness of fit of the least-squares linear regression between $h_S$ and $\varepsilon$90 GHz (V) and $T_B$ 90 GHz (V) are:

$$\varepsilon 90\ \text{GHz (V)} = 1.08 - 0.019 * h_S\ \text{(cm)} \qquad (n = 10,\ r^2 = 0.78) \qquad (1)$$

$$T_B 90\ \text{GHz (V)} = 290.24 - 5.21 * h_S\ \text{(cm)} \qquad (n = 10,\ r^2 = 0.77) \qquad (2)$$

Measurements with vertical polarization were more strongly correlated with $h_S$ than those with horizontal polarization, which had higher (by ~10%) standard deviations. The number of stations where measurements at vertical polarization were taken was higher as well. The linear regression of the $h_S$ data from Comiso et al. (1989) was

$$T_B 90\ \text{GHz (V)} = 257.89 - 1.06 * h_S\ \text{(cm)} \qquad (n = 4,\ r^2 = 0.99) \qquad (3)$$

and is shown in Fig. 6 along with the data used to generate Eq. (2). Equation (2) has a much steeper slope than Eq. (3), suggesting that predictions of $h_S$ made using Eq. (2) will be more sensitive to changes in T90 GHz (V). Also, if the measured $T_B$ is below 250°K, Eq. (2) will

predict lower values of $h_S$, while at $T_B$ above 250°K Eq. (2) will give higher values. At T 250°K, both algorithms produce a similar value for $h_S$ (~0.08 m).

If the relationship between $h_S$ and microwave signal is expanded to include two frequencies, 90 GHz (V) and either 18.7 GHz (V) or 10 GHz (V), the regression improves further still

$$\varepsilon 90\text{ GHz (V)} - \varepsilon 10\text{ GHz (V)} = 0.20 - 0.0227 * h_S\text{ (cm)} \quad (n=11, r^2=0.92) \quad (4)$$

$$T_B 90\text{ GHz (V)} - T_B 10\text{ GHz (V)} = 55.56 - 6.20 * h_S\text{ (cm)} \quad (n=12, r^2=0.92) \quad (5)$$

$$\varepsilon 90\text{ GHz (V)} - \varepsilon 18.7\text{ GHz (V)} = 0.13 - 0.0197 * h_S\text{ (cm)} \quad (n=12, r^2=0.89) \quad (6)$$

$$T_B 90\text{ GHz (V)} - T_B 18.7\text{ GHz (V)} = 35.91 - 5.43 * h_S\text{ (cm)} \quad (n=12, r^2=0.90) \quad (7)$$

The advantage of this approach was that, in contrast to Eqs. (1) and (2) where snow-free stations were omitted, stations where $h_S = 0$ m fitted the resulting regression well (Fig. 7). Thus, the algorithms shown in Eqs. (4-7) apply to all cases where $h_S < 0.25$ m. This restriction is because of the fact that at higher values of $h_S$, the penetration depth of radiation at 90 GHz is smaller than the snow depth itself (Hall & Martinec 1985).

Only Eqs. (6) and (7) can be applied to SSM/I satellite data to generate estimates of $h_S$ because unlike SMMR, SSM/I does not have a 10 GHz channel. SSM/I does not have a 90 GHz channel either, but it is expected that the differences between the data generated from the 85 GHz frequency of the SSM/I and the 90 GHz field data will be small enough to allow substitution of the 85 GHz SSM/I data into Eqs. (6) and (7).

Foster and Chang (1993) developed a simple algorithm to predict $h_S$ on land using the microwave brightness temperatures at 18 and 37 GHz. Their equation was

$$h_S = 1.59 * [T_B 18\text{ GHz (H)} - T_B 37\text{ GHz (H)}] \quad (8)$$

However, this algorithm provided a poor fit to the sea ice data, perhaps because of the different emissivities of land and ice.

ANT VIII/2 (1989)

During the Weddell Sea Experiment, $h_S$ and surface based radiometer measurements were taken simultaneously at 18 stations at an angle 50° from nadir from September 16 to October 6, 1989. Unlike 1986, only 10 GHz (V and H polarization) and 85 GHz (V and H polarization) frequencies

were measured. Although more detailed information of the snow cover was reported (grain size, vertical structure of the snow layer, presence of ice lenses, etc.), mean $h_s$ at each station was determined from, at most, four measurements within the radiometer footprint. Snow depths ranged from 0.08 to 0.61 m and were generally less variable than in 1986. Most of the thick snow cover was observed in the western Weddell Sea where the ice cover is generally thicker. Standard deviations for a specific station could be >100% of the mean $h_s$, but were generally <40%.

Plotting the 85 GHz versus the 10 GHz frequency conformed to expectations; $T_B$ at 10 GHz was fairly constant, while the signal at 85 GHz was highly variable. Also, $T_B$ and $\varepsilon$ for the 10 GHz channel were highly linearly correlated ($r^2$>0.99) (Fig. 8A). However, $T_B$ and $\varepsilon$ were poorly correlated for the 85 GHz band for both H and V polarization (Fig. 8B). This observation was in direct contrast to measurements made in 1986 which showed a highly linear relationship (Fig. 2) and suggests that the sky calibration of the radiometer in 1989 was not as good as those in 1986. However, some of the 1989 data conform to the relationship between $T_B$ and e found in the 1986 data. When the line of best fit from 1986 (Fig. 2) is plotted with the 1989 data, some of the points lie along the regression (Fig. 8B), suggesting that the calibration for these points may be correct. It is interesting to note that all of the suspect data lie to the right of the 1986 regression line.

Because of the calibration problem, $h_s$ was poorly correlated with the quantity ($\varepsilon$85-$\varepsilon$10) GHz (V) in the 1989 data set (Fig. 9). However, if the line of best fit of this relationship from the 1986 data is plotted with the data from 1989, it can be seen that some of the 1989 data points lie on or near the 1986 regression line. Interestingly, the 1989 data points that conform to the 1986 relationship between $T_B$85 GHz and $\varepsilon$85 GHz also conform to the 1986 relationship between $h_s$ and the quantity ($\varepsilon$85-10) GHz (V) (see circled solid black data points on Figs. 8 and 9). There were four other stations in 1989 which conform to the 1986 relationship between $T_B$ 85 GHz and $\varepsilon$85 GHz but do not fit the 1986 relationship between hs and the quantity ($\varepsilon$85-10) GHz (V). Therefore, the fact that $T_B$ and $\varepsilon$ at a particular station relate as expected cannot be used as a proxy for "good data" for the snow depth algorithm. On the other hand, the disagreement of those data with the algorithm could be caused by experimental or weather conditions as well. For example, the header of these data files contained comments such as: "probably moist snow surface," "radiometers may not be warm enough yet," "cloud broken/sun in and out station," and "near white out start of angular scan, slow motion work to be done at the end"; conditions which would very likely affect the microwave signature.

Comparisons with SSM/I data

Eqs. (6) and (7) were used to predict $h_S$ in the Weddell Sea from SSM/I imagery. The mean value for $h_S$ estimated from SSM/I data was nearly identical to that calculated from >1400 in situ measurements. However, the frequency histograms exhibited different distributions, with the in situ data exhibiting a lognormal distribution and the estimates from SSM/I tending toward a more normal distribution (Fig. 10). The differences in the two distributions is not surprising, however. The Central Limit Theorem states that the sampling distribution of the mean approaches the normal distribution as the sample size increases, regardless of the shape of the distribution of the raw data. In our case, the SSM/I averages the snow depth over an area of 625 $km^2$, which is essentially the same as increasing the sample size, resulting in a normal distribution. Despite the differences in distribution, the agreement between the means of the two data sets suggests that the algorithm is able to provide a reasonable estimate of $h_S$ from SSM/I satellite data over a large area.

**ACKNOWLEDGMENTS**: This work was supported by a Maryland Sea Grant College/NASA fellowship in Remote Sensing of the Oceans to G. van Dijken.

## REFERENCES

1. Carsey, F.D., R.G. Barry and W.F. Weeks. 1992. Introduction. In: F.D. Carsey [ed.], *Microwave Remote Sensing of Sea Ice, Geophys. Monogr. Ser. 68:1-7,* AGU, Washington, D.C.
2. Comiso, J.C., T.C. Grenfell, D.L. Bell, M.A. Lange and S.F. Ackley. 1989. "Passive microwave in situ observations of winter Weddell Sea ice," *J. Geophys. Res. 94(C8):* 10,891-10,905.
3. Foster, J.L. and A.T.C. Chang. 1993. "Snow cover," In: R.J. Gurney, J.L. Foster and C.L. Parkinson [eds.], *Atlas of satellite observations related to global change.* Cambridge University Press, New York, p. 361-370.
4. Grenfell, T.C., J.C. Comiso, M.A. Lange, H. Eicken and M.R. Wensnahan. 1994. "Passive microwave observations of the Weddell Sea during austral winter and early spring," *J. Geophys. Res. 99(C5):* 9,995-10,010.
5. Hall, D.K. and J. Martinec. 1985. *Remote Sensing of Ice and Snow,* Chapman and Hall, New York. 189 pp.

# FIGURES

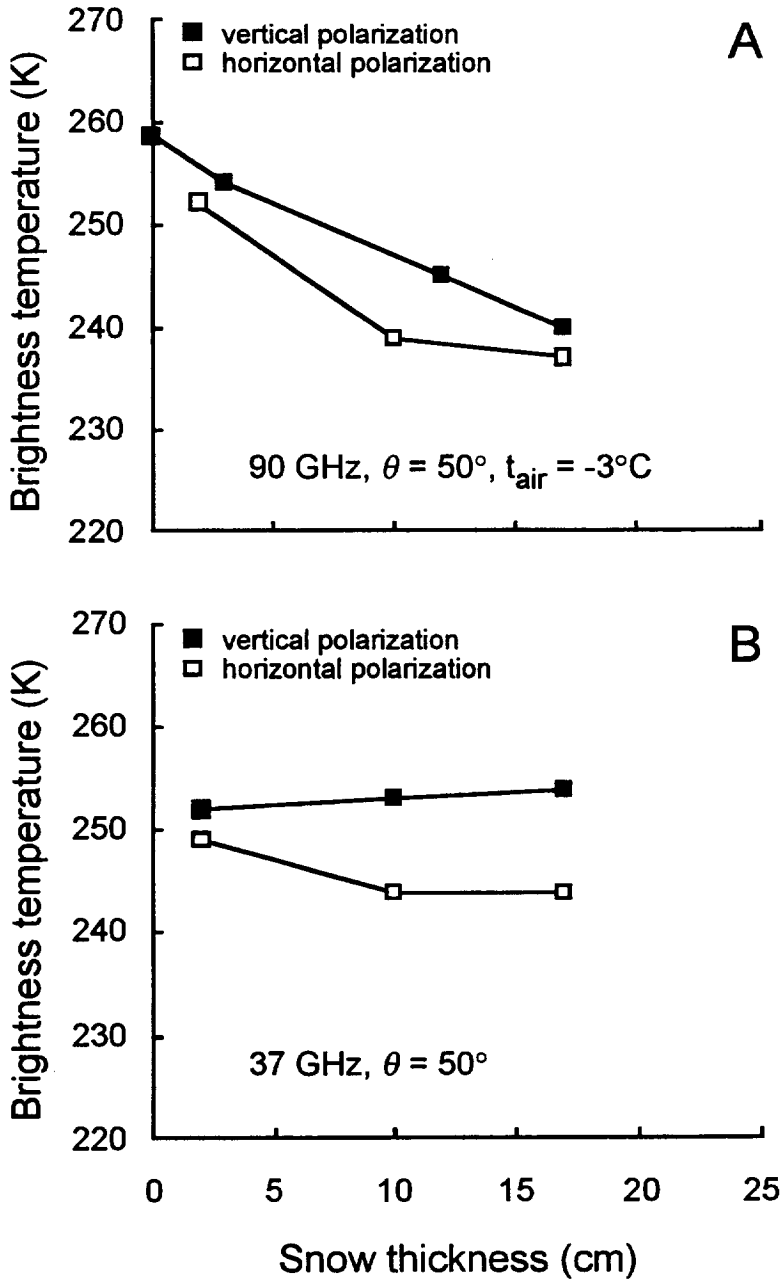


Figure 1. Brightness temperature at 90 and 37 GHz as a function of snow depth. Data was collected using a microwave radiometer mounted ~1.5 m. above the sea ice in an area of substantial snow cover. Radiometric measurements were made as the snow was carefully scraped off in layers of 0.05 m.

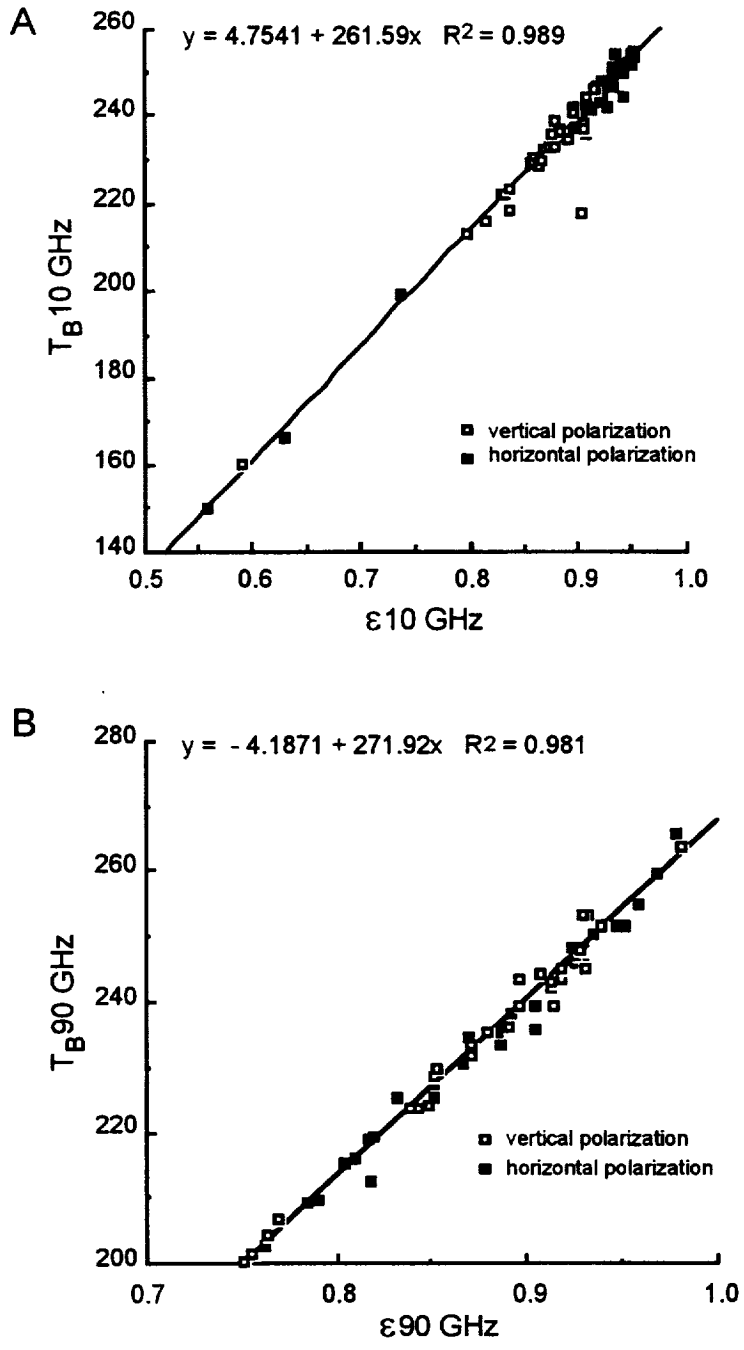


Figure 2. Brightness temperature versus emissivity at frequencies of (A) 10 GHz and (B) 90 GHz. Data was collected in 1986 as described in Fig. 1 with the exception that the radiometer was mounted on the RV Polarstern ~17 m above the ice surface.

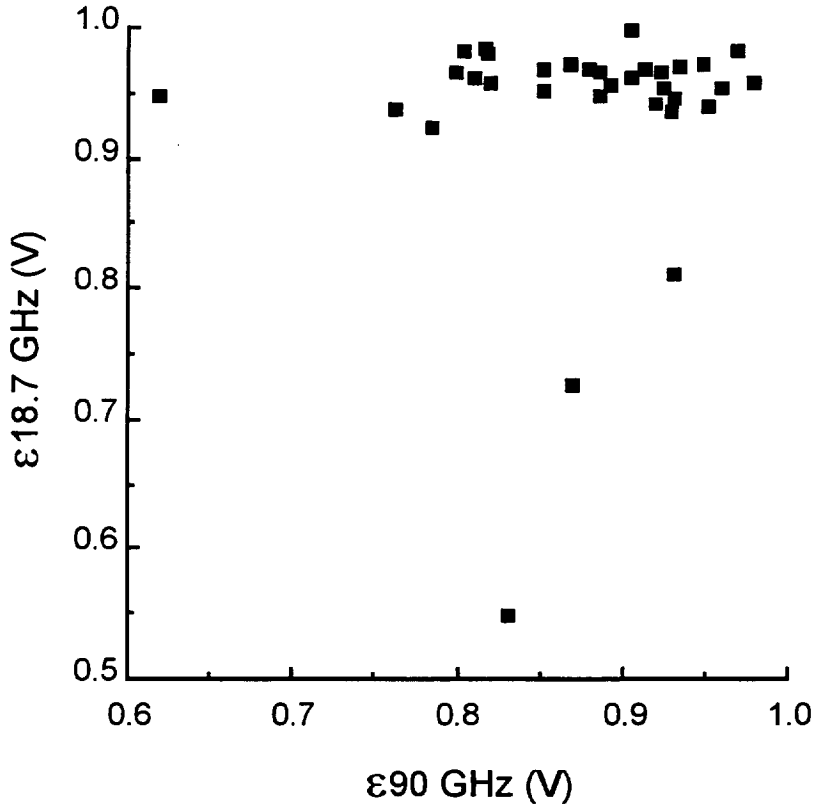


Figure 3. Emissivity at 18.7 GHz versus emissivity at 90 GHz. Data was collected as described in Fig. 2.

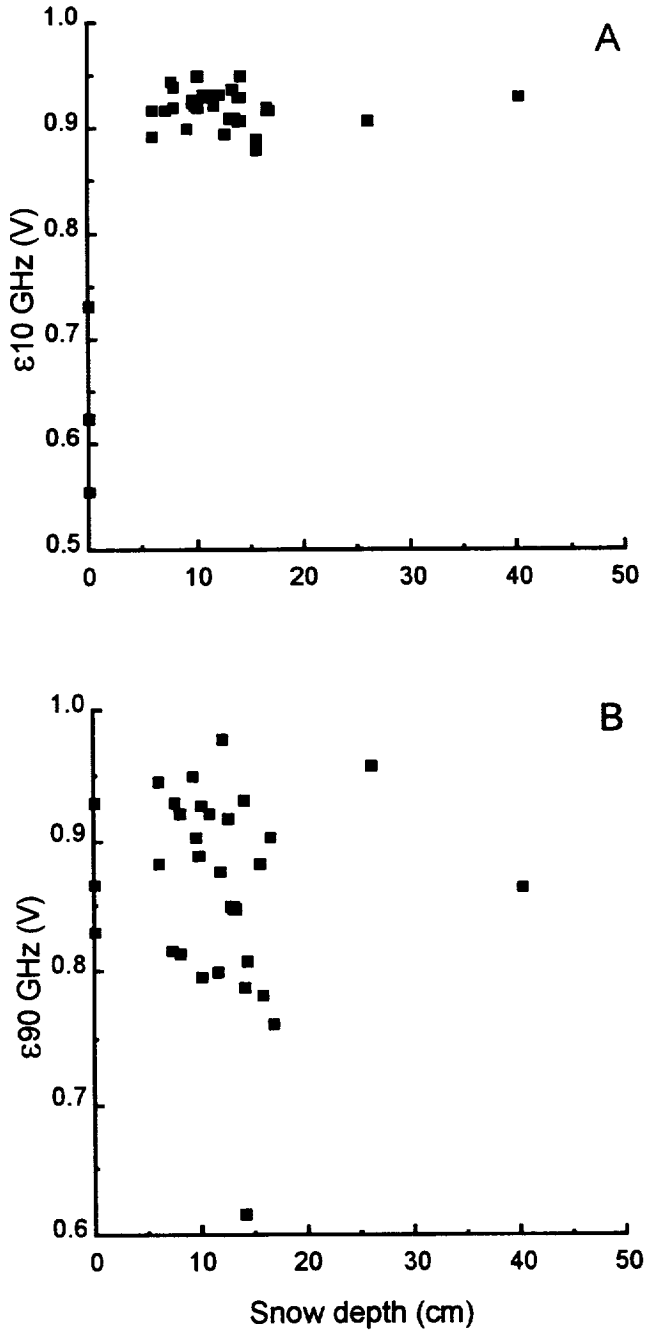


Figure 4. Snow depth versus emissivity at frequencies of (A) 10 GHz and (B) 90 GHz. Data was collected as described in Fig. 2.

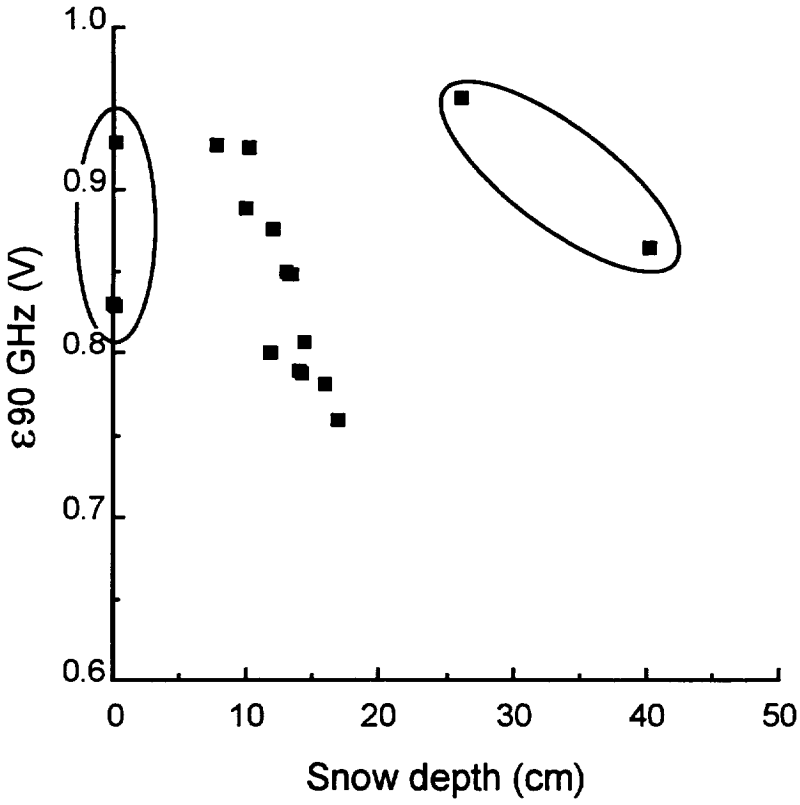


Figure 5. Snow depth versus emissivity at 90 GHz after removing data points where the standard deviation of the snow depth was <50% of the mean. Circled data points indicate where $h_S = 0$ and $h_S > 0.25$ m. Data was collected as described in Fig. 2.

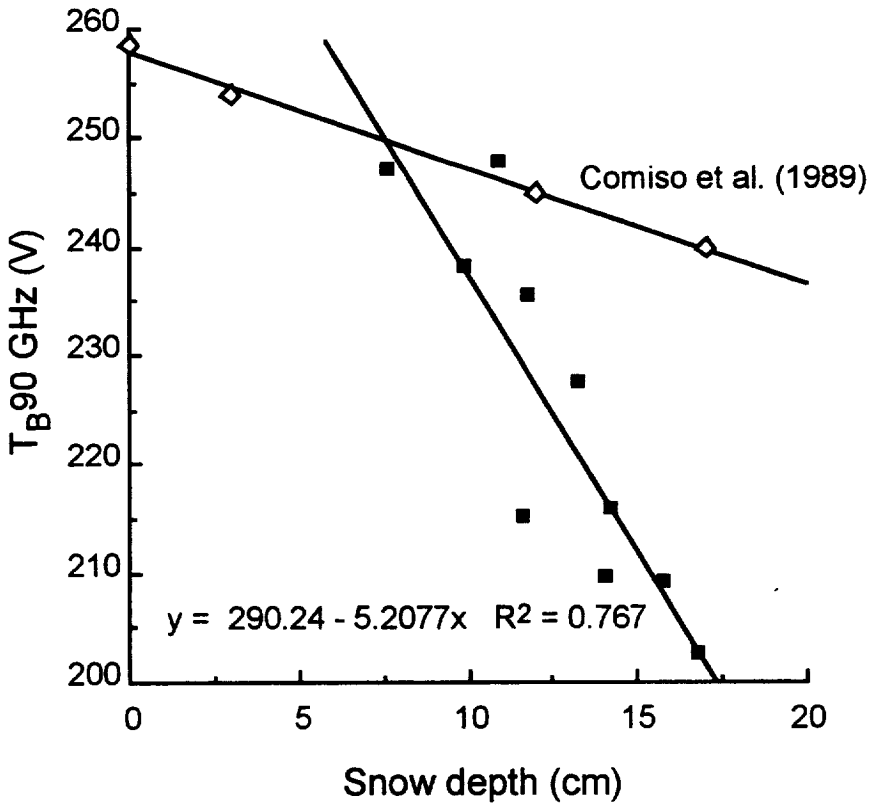


Figure 6. Least-squares regression of brightness temperature at 90 GHz versus snow depth (closed squares). Data points where the standard deviation of the snow depth was <50% of the mean, and where $h_S = 0$ and $h_S > 0.25$ m were also omitted. The best fit line of the data from Comiso et al. (1989) is shown for comparison (open diamonds). Data was collected as described in Fig. 2.

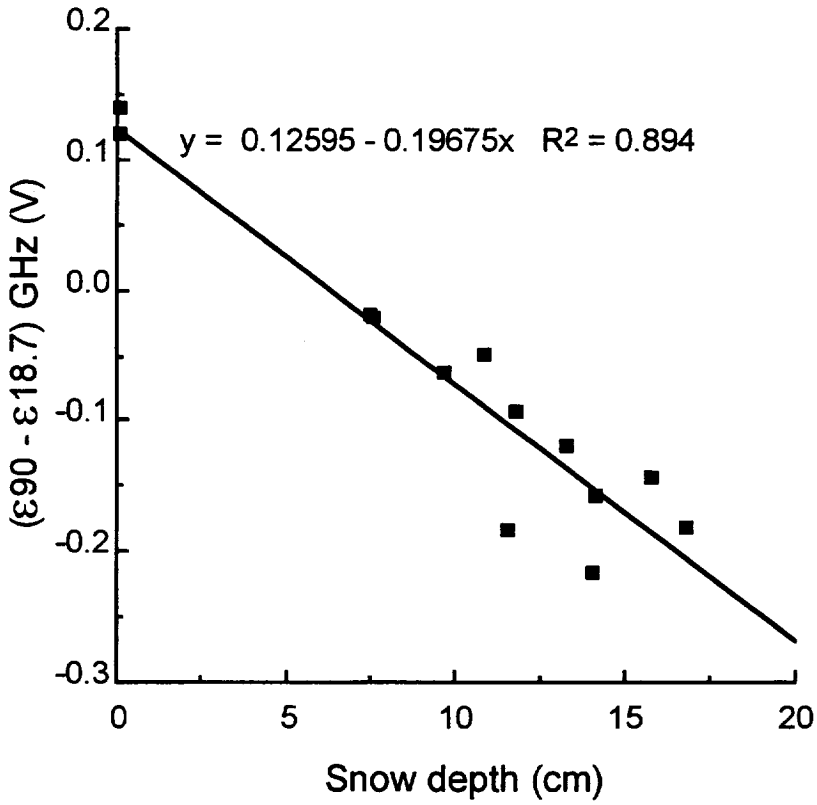


Figure 7. Snow depth versus the difference in emissivity at 90 GHz and 18.7 GHz. Note that data points where $h_S = 0$ m have now been included. Data was collected as described in Fig. 2.

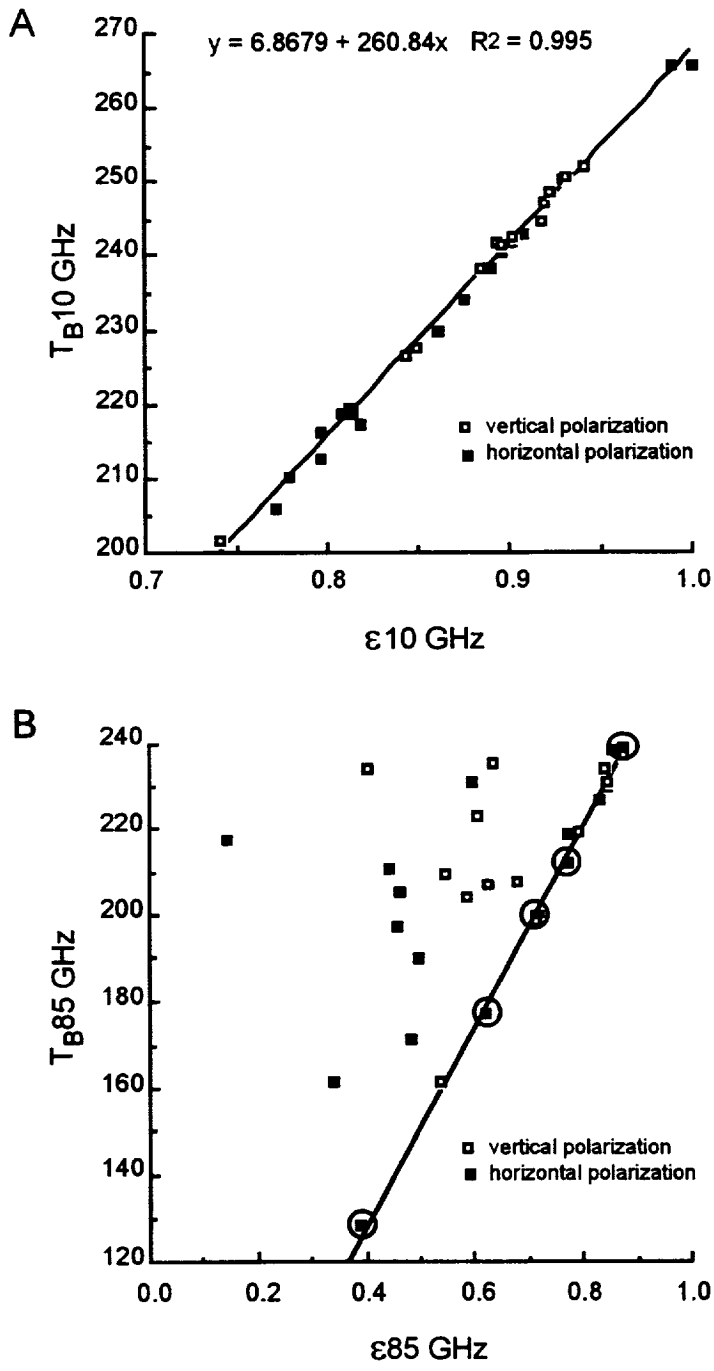


Figure 8. Brightness temperature versus emissivity at frequencies of (A) 10 GHz and (B) 90 GHz. Data was collected in 1989 as described in Fig. 1 with the exception that the radiometer was mounted on the RV Polarstern ~17 m above the ice surface. The line in (B) is the least squares fit to the 1986 data shown in Fig. 2B. Circled data points in (B) correspond to circled data points in Fig. 9 and indicate data which may be salvageable.

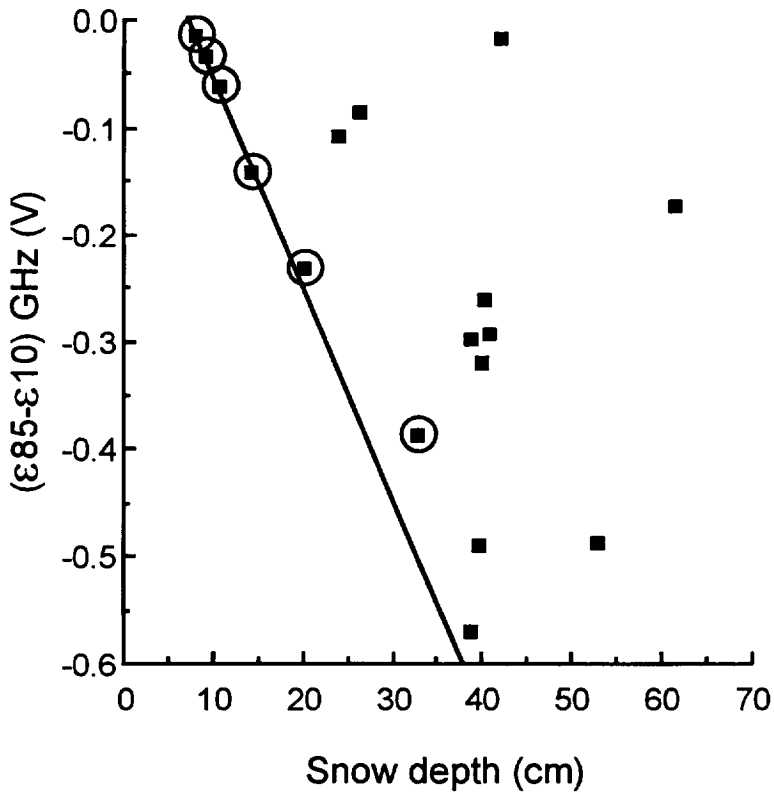


Figure 9. Snow depth versus the difference in emissivity at 85 GHz and 10 GHz. The line is the least squares fit to the 1986 data shown in Fig. 7. Data was collected as described in Fig. 8.

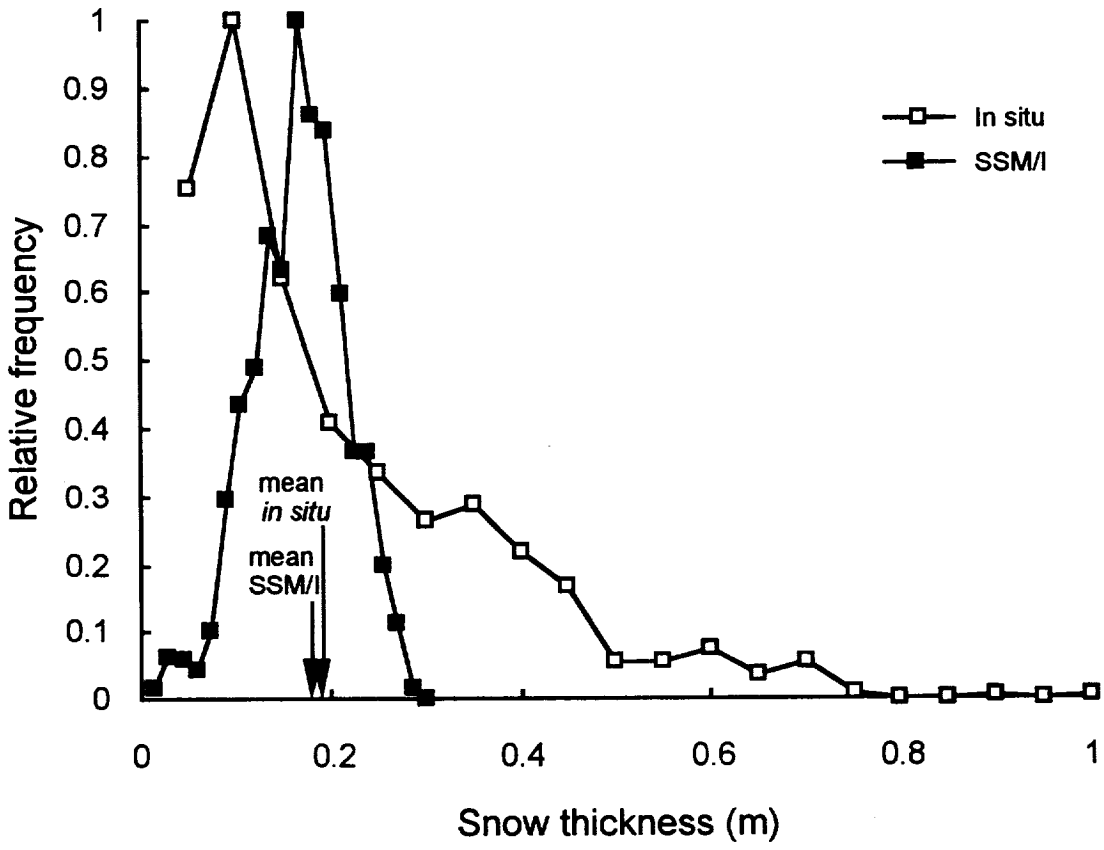


Figure 10. Comparison of the relative frequency distributions of snow depth as determined from in situ data and from estimates made using SSM/I data as input to Eq. (6). Note that the means for the two methods are almost identical. Differences in the distributions are explained in the text.

# REPORT DOCUMENTATION PAGE

*Form Approved*
*OMB No. 0704-0188*



| 1. AGENCY USE ONLY *(Leave blank)* | 2. REPORT DATE | 3. REPORT TYPE AND DATES COVERED |
|---|---|---|
| | December 1996 | Technical Memorandum |

**4. TITLE AND SUBTITLE**

Estimating the Thickness of Sea Ice Snow Cover in the Weddell Sea from Passive Microwave Brightness Temperatures

**5. FUNDING NUMBERS**

Code 971

**6. AUTHOR(S)**

K. R. Arrigo, G. L. van Dijken, and J. C. Comiso

**7. PERFORMING ORGANIZATION NAME(S) AND ADDRESS(ES)**

Laboratory for Hydrospheric Processes
Goddard Space Flight Center
Greenbelt, Maryland 20771

**8. PERFORMING ORGANIZATION REPORT NUMBER**

97B00003

**9. SPONSORING/MONITORING AGENCY NAME(S) AND ADDRESS(ES)**

Goddard Space Flight Center
National Aeronautics and Space Administration
Washington , DC 20546-0001

**10. SPONSORING/MONITORING AGENCY REPORT NUMBER**

TM-104640

**11. SUPPLEMENTARY NOTES**

G. L. van Dijken: Department of Oceanography, Texas A&M University, College Station, TX 77843-3146

**12a. DISTRIBUTION/AVAILABILITY STATEMENT**

Unclassified-Unlimited
Subject Catagory: 43
This report is available from the NASA Center for AeroSpace Information, 800 Elkridge Landing Road, Linthicum Heights, MD 21090; (301) 621-0390

**12b. DISTRIBUTION CODE**

**13. ABSTRACT** *(Maximum 200 words)*

Passive microwave satellite observations have frequently been used to observe changes in sea ice cover and concentration. Comiso et al. (1989) showed that there may also be a direct relationship between the thickness of snow cover ($h_s$) on ice and microwave emissivity at 90 GHz. Because the in situ experiment of experiment of Comiso et al. (1989) was limited to a single station, the relationship is re-examined in this paper in a more general context and using more extensive in situ microwave observations and measurements of $h_s$ from the Weddel Sea 1986 and 1989 winter cruises. Good relationships were found to exist between $h_s$ and the emissivity at 90 GHz–10 GHz and the emissivity at 90 GHz–18.7 GHz when the standard deviation of $h_s$ was < 50% of the mean and when hs was < 0.25 m. The reliance of these relationships on $h_s$ is most likely caused by the limited penetration through the snow of radiation at 90 GHz. When the algorithm was applied to the Special Sensor Microwave/Imager (SSM/I) satellite data from the Weddell Sea, the resulting mean $h_s$ agreed within 5% of the mean calculated from > 1400 in situ observations.

**14. SUBJECT TERMS**

Antarctica, snow, SSM/I, passive microwave

**15. NUMBER OF PAGES**

20

**16. PRICE CODE**

| 17. SECURITY CLASSIFICATION OF REPORT | 18. SECURITY CLASSIFICATION OF THIS PAGE | 19. SECURITY CLASSIFICATION OF ABSTRACT | 20. LIMITATION OF ABSTRACT |
|---|---|---|---|
| Unclassified | Unclassified | Unclassified | Unlimited |